[1.] Camil CRĂCIUN, [2.] Traian MAZILU

ON THE LONGITUDINAL DYNAMICS OF THE BRAKED FREIGHT TRAINS WITH MULTIPLE TRACTION

[1-2.] University POLITEHNICA of Bucharest, Faculty of Transports, Department of Railway Rolling Stock, Bucharest, ROMANIA

Abstract: The paper introduces the analysis of the distribution on the collision, traction and coupling equipment of the longitudinal dynamic forces developed in the body of the freight trains with multiple traction under the braking behavior. The study has considered two types of train forming: a 40-coach freight train and two locomotives – the traction locomotive and push locomotive located behind the train and another model, comprising a third locomotive in the middle of the train. The trains are subjected to an emergency braking action from the maximum speed of 100 km/h. These models will help examine the influence of the coach weights upon the longitudinal dynamic forces.
Keywords: longitudinal dynamics of train, brakes, traction, collision and coupling devices, freight trains

1. INTRODUCTION

During the braking of the freight trains, longitudinal dynamic forces occur in the traction, collission and coupling equipment, due to the differences between the braking forces developed on each train coach, as a result of the successive proceeding of the individual braking devices. These longitudinal dynamic forces place a stress upon the coach bearing structure and generate shocks that can affect the integrity of the transported goods and, in some cases, the running safety.

The main purpose of the studies on the longitudinal dynamics of trains refers to identifying the means of decreasing the longitudinal forces present during the braking of the trains.

Among the first studies on the longitudinal dynamics in the freight trains, the list includes *Duncan & Webb* [1], or *Jolly & Sismey* [2]. *Nasr* & *Mohammadi* [3] examines the effect of the delay in the development of the braking forces upon the longitudinal dynamics in the freight trains, via numerical simulations. Three values of the delay time of the proceedings of the air distributors are being considered. The model in use to evaluate the longitudinal forces is non-linear, similar to the one suggested by Cole [4], which describes the friction between the elastic elements and of damping in the automatic coupling.

Fukazawa [5] determines the dynamic forces in the traction, collision and coupling equipment for the two-axle freight trains, reaching to the conclusion that the emergency braking is not necessary for speeds lower than 30 km/h in order to avoid the emergence of the large compression forces in these devices.

Zobory & *Bekefi* [6] introduces a numerical simulation program of the longitudinal dynamic forces developing in the body of the trains both during the traction and also the braking behaviors.

A thorough study on the longitudinal dynamics in the freight trains using various non-linear models is conducted by *Ansari et al* [7]. The authors are dealing with the influence of diverse factors, such as the rigidity and damping of the automatic couplers, the train speed and acceleration, the distribution of the weights in the train body upon the longitudinal dynamic behavior. Similarly, the authors raise the issue of the positioning of an empty coach in the train body, so as to notice the effects upon the longitudinal dynamic forces.

Pugi et al [8] deals with the issue of the influence of the airwave propagation upon the longitudinal dynamic forces for the freight train under emergency braking, thus explaining that the emergence of the variable braking forces are the cause of the longitudinal forces that can lead to the damage in the traction, collision and coupling devices and even to the coach derailment.

Stoica [9] has drafted a calculation program for the longitudinal dynamic forces emerging in the body of the freight trains during braking. In order to be able to determine the braking force for each coach, it is necessary to know the pressure variation in time for each braking cylinder in the train body. The program calculates the balanced longitudinal forces, by which the values of the experimentally determined forces can be interpreted.

This paper features an analysis of the distribution of the maximum longitudinal forces of compression and extension developing the traction, collision and coupling devices during the braking of the freight trains with multiple traction.

2. THE TRAIN MECHANICAL MODEL

To study the longitudinal dynamic effects in the body of a train under braking, the mechanical model in figure 1 will be adopted. This comprises n rigid bodies of a weight m_i, $i = 1 .. n$, representing the train wagons, connected via the collision, traction and coupling devices [12, 13]. Two types of train forming have been taken into account:

✓ a 40-wagon freight train, the traction locomotive and the push locomotive located at the end of the train - Lo-40W-Lo (see Figure 1 a);

✓ a 40-wagon freight train, a traction locomotive and two push locomotives located in the midlde and at the end of the train, respectively - Lo-20W-Lo-20W-Lo (see Figure 1 b).

The following simplifying hypotheses have been selected:

✓ all the wagons are equipped with a slow-action break and the air distributors in the train body provide the same filling characteristic;

✓ the initial compression of the elastic elements of the collision and traction devices is neglected;

✓ there is no clearance left between the wagons, according to the stipulations for the freight trains [14];

✓ the average propagation speed of the braking wave along the train is of 250 m/s, i.e. the minimum value required by the regulations [15] ;

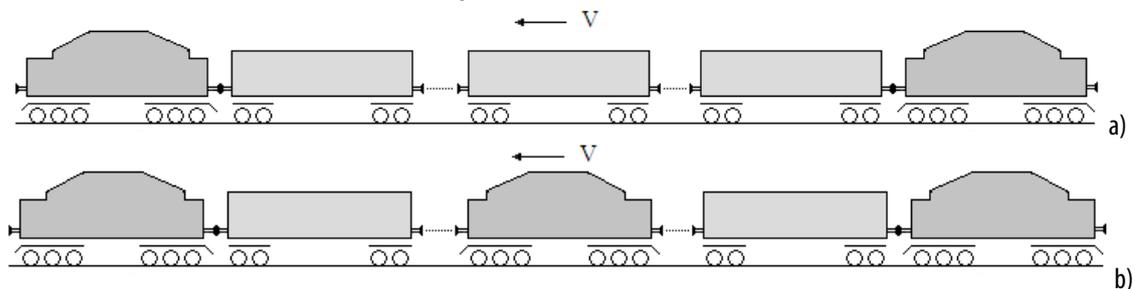✓ the adherence coefficient is the same for all the wagons in the train.

Figure 1. The model of the train: a) train with a traction locomotive and the push locomotive, b) train with a traction locomotive and two push locomotives

The maximum braking force developed by each wagon should not exceed the wheel-rail adherence force, in order to avoid the blocking of axles during a normal operation of the brake [12, 13]. Under these conditions, at any time moment t, the braking force of the wagon i in the train, $F_{fi}(t)$, which is smaller or at most equal with the maximum braking force of the wagon, F_{fmaxi}, meets the below requirement:

$$F_{fi}(t) \leq F_{fmaxi} = \mu_a \cdot m_i \cdot g \qquad (1)$$

where μ_a is the wheel-rail adherence coefficient, m_i is the vehicle weight i, and g is the gravitational acceleration.

On the other hand, the braking force is proportionate to the instantaneous pressure in the braking cylinder of the vehicle, $p_{cfi}(t)$, according to the equation:

$$F_{fi}(t) = F_{fmaxi} \frac{p_{cfi}(t)}{p_{cfmax}} = \mu_a \cdot m_i \cdot g \frac{p_{cfi}(t)}{p_{cfmax}} \qquad (2)$$

where p_{cfmax} is the maximum pressure developed in the braking cylinders.

The instantaneous pressure in the braking cylinder can be experimentally determined on a computer-based testing stand for the braking equipment [13].

Figure 2 shows such an example of the pressures in the braking equipment during the emergency braking with the behavior exchanger in the position G.

To determine the static and dynamic characteristics in the collision devices, *Sârb* [10] conducts experimental determinations on Ringfeder-type metallic ring buffers and rubber elements buffers, according to the UIC 526-1leaflet [11]. Further on, the diagram specific to the buffer equipping the towed freight vehicles, built in Romania, will be taken into account (Figure3).
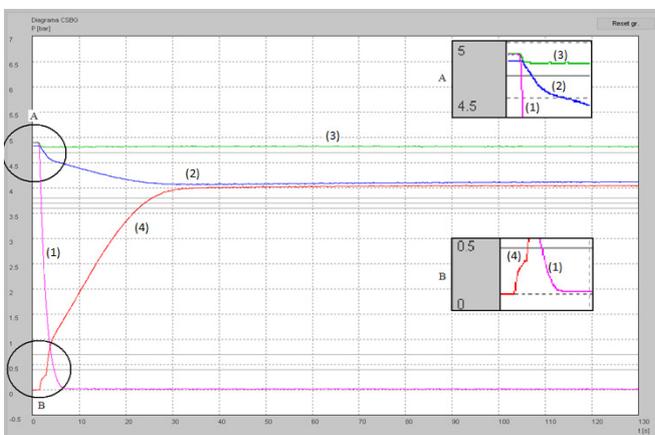

Figure 2. The pressure in the braking devices (emergency braking): (1) in the main pipeline; (2) in the auxiliary reservoir; (3) in the operating room of the air distributor; (4) in the braking cylinder [16].

The deformation force of the buffer depends on the variation of the displacement and the relative velocities between the vehicles, the rigidity of the elastic elements as well as on the damping degree.

As a consequence, the calculation of the forces in the traction, collision and coupling devices can be done via the equation [16]:

$$F(x,\dot{x}) = \begin{cases} k_e \cdot x + k_f \cdot |x| \cdot \tanh(u \cdot \dot{x}) & \text{for } x < 0, \\ 0 & \text{for } x = 0, \\ k_{ec} \cdot x + k_{fc} \cdot |x| \cdot \tanh(u \cdot \dot{x}) & \text{for } x > 0 \end{cases} \tag{3}$$

where x is the stroke, $\dot{x}$ the speed in these devices, k_{ec} and k_{fc} the coefficients describing the elasticity and friction in the buffer elements and u is a scaling factor.

Due to the fact that the vehicles are equipped with traction and coupling devices during exploitation, with elastic and damping elements that are similar to the collision ones, the mathematical model identical with the buffers' has been considered, while looking at the coefficients describing the elasticity k_{ec} and the friction k_{fc} specific to these devices.

Thus, the relation (3) can be used to simulate the operating of the traction, collision and coupling devices and generates the characteristic in figure 4, where for $x > 0$ only the collision device will start functioning, at $x = 0$ the force will be zero for the collision and coupling and for $x < 0$, only the traction and coupling device will be operational.
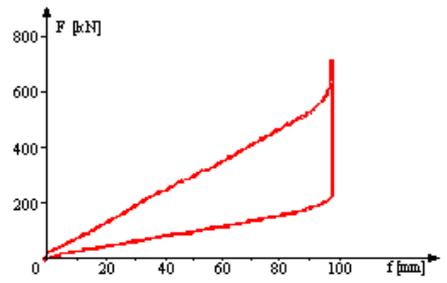

Figure 3. The characteristic of the Ringfeder-type buffer used on freight trains, [10].

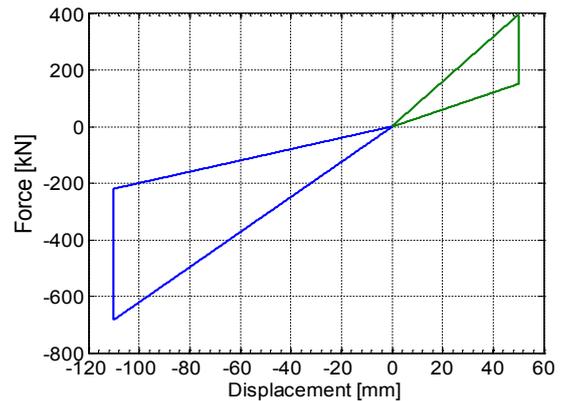**Figure 4.** The force-stroke characteristic diagram for the traction, collision and coupling RINGFEDER type device fitting the passenger trains

3. THE GENERAL MOVEMENT EQUATIONS

For the model of the train featured in figure 1, the following movement equations can be written:

$$m_1 \cdot \ddot{x}_1 = -F_1(\Delta x_1, \Delta \dot{x}_1) - F_{f1}(t) - R_1(v(t))$$
$$m_2 \cdot \ddot{x}_2 = -F_2(\Delta x_2, \Delta \dot{x}_2) + F_1(\Delta x_1, \Delta \dot{x}_1) - F_{f2}(t) - R_2(v(t))$$
$$m_3 \cdot \ddot{x}_3 = -F_3(\Delta x_3, \Delta \dot{x}_3) + F_2(\Delta x_2, \Delta \dot{x}_2) - F_{f3}(t) - R_3(v(t))$$
$$\dots\dots\dots\dots\dots\dots\dots\dots\dots\dots\dots\dots\dots\dots\dots\dots\dots$$
$$m_i \cdot \ddot{x}_i = -F_i(\Delta x_i, \Delta \dot{x}_i) + F_{i-1}(\Delta x_{i-1}, \Delta \dot{x}_{i-1}) - F_{fi}(t) - R_i(v(t)) \tag{4}$$
$$\dots\dots\dots\dots\dots\dots\dots\dots\dots\dots\dots\dots\dots\dots\dots\dots\dots\dots\dots\dots$$
$$m_{n-1} \cdot \ddot{x}_{n-1} = -F_{n-1}(\Delta x_{n-1}, \Delta \dot{x}_{n-1}) + F_{n-2}(\Delta x_{n-2}, \Delta \dot{x}_{n-2}) - F_{fn-1}(t) - R_{n-1}(v(t))$$
$$m_n \cdot \ddot{x}_n = F_{n-1}(\Delta x_{n-1}, \Delta \dot{x}_{n-1}) - F_{f,n}(t) - R_n(v(t)),$$

where $\ddot{x}_i$ is the acceleration of the vehicle i, x_i is the relative displacement between vehicles i and $i+1$, $F_i(\Delta x_i, \Delta \dot{x}_i)$ - the force between the vehicles i and $i+1$, and $R_i(V(t))$ – the rolling resistance of the vehicle i that depends on the instantaneous speed $V(t)$, expressed in km/h.

The rolling resistance of the coaches in the train body can be calculated via the equation:

$$R_i = m_i \cdot g \cdot r_i \tag{5}$$

where r_i is the specific rolling resistance of the vehicle i.

The specific rolling resistances are a function of the coach type and can be determined by means of the following empirical equations [16]:

☐ for regular freight coaches (in a mixed combination):

$$r = 2 + \frac{V^2(t)}{1950} \tag{6}$$

☐ for electric locomotives:

$$r = \frac{1}{120} \cdot \left[296 \cdot 7.068 \cdot \left[\frac{V(t)}{10} \right]^2 \right]. \tag{7}$$

Upon integrating the movement equations, the longitudinal forces in the traction, collision and coupling devices will be calculated via the relation (3).

4. NUMERICAL APPLICATION

This section includes the effect of an emergency braking applied at the velocity of 100 km/h to a freight train with multiple traction. The train is considered to be formed of locomotives of 100 t in weight, while three values are being taken into account for the weight of the wagons:

50 t, 65 t and 80 t, respectively.

The main parameters in use are:

✓ for the collision devices (buffers), the constant depending on the elastic elements $k_e = 4.1 \cdot 10^6$ N/m and the constant depending on the friction force $k_f = 2.1 \cdot 10^6$ N/m;

✓ for the traction and coupling devices (the mechanical coupling and the traction hook), the constant depending on the elastic elements $k_{ec} = 5.46 \cdot 10^6$ N/m and the constant depending on the friction force $k_{fc} = 2.43 \cdot 10^6$ N/m;

✓ the adherence coefficient $\varphi_a = 0.1$;

✓ the value of the scaling factor $u = 10^4$ [12, 16].

As input data for the simulation program, there will be: the pressure in the braking cylinders, the constants depending on the elastic and friction elements for the traction, collision and coupling devices, the weights of the coaches in the train body, the delay in the brake proceeding, the maximum train velocity where the emergency braking starts from, the integration time. The output data of the program are the following: the displacement and the relative velocity between the consecutive coaches, the time-based evolution of the longitudinal forces in the traction, collision and coupling devices, as well as the maximum values of the compression and extension in such devices.

The figures 5 and 6 feature the time evolution of the relative displacement and of the longitudinal forces between the consecutive wagons for the train with two locomotives and wagons of 65-tone in weight.

Even from the beginning, the emergence of the relative time-lagged displacement between the consecutive wagons is present, due to the large length of the main air pipeline, triggering the delay in the local decrease of the pressure in each air distributor in the train body. Similarly, the filling time of the braking cylinder for the slow-action brake, specific to the freight trains, directly influences the time variation of the relative displacements. During the pressure increase in each brake cylinder, the compression of the collision devices between the coaches is visible (also the compression of

Figure 5. The relative displacements between wagons.

Figure 6. The longitudinal forces between wagons

the entire train) and reaches the maximum value during the second stage of braking when the differences in the braking forces between the wagons are at the highest (the braking force in the first wagon reaches the maximum braking force).

According to the figures 5 and 6, the maximum train compression triggers a longitudinal force in the collision devices, which reaches the value of 205 kN.

As the pressures in the braking cylinders start equalizing with one another and acquire the maximum value (specific to the third stage of braking), a decompression of the train is visible in chart 5 for the interval 25…27 where the relative displacement shows an increase towards the balance position (the zero position or the coupling position of the coaches). This aspect is also visible in the evolution of the longitudinal forces in figure 6.
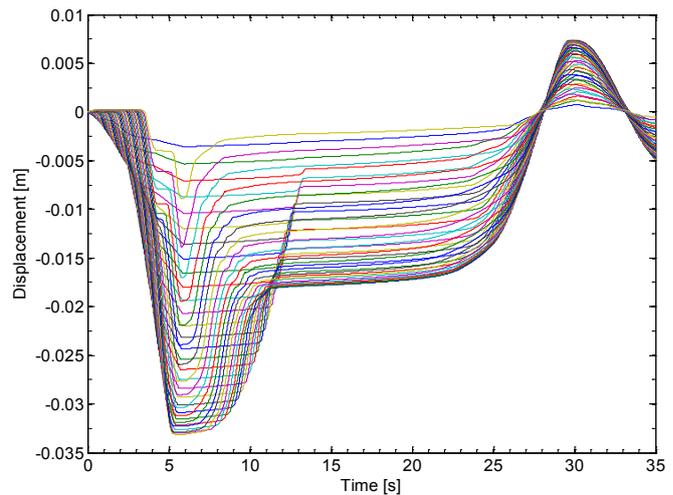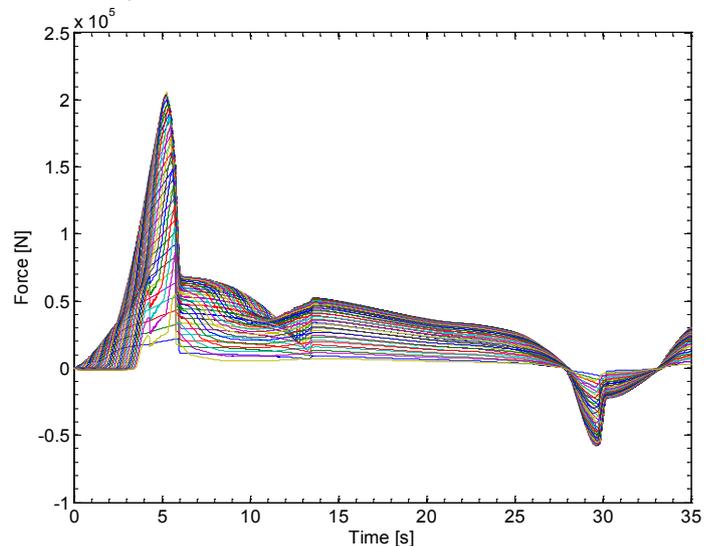
After the maximum pressure has been reached in all the braking cylinders (the fourth stage of braking), the train rebound shows, described by the train extension and the tendency of increasing the relative displacement between wagons, thus making the traction and coupling devices operational. As a result of their elasticity, the train will be again compressed after circa 33 seconds after the initiation of the emergency braking.

To notice the differences for the two types of trains under study (two-locomotive and three-locomotive) and also the influence of the weight of the wagons upon the longitudinal dynamics, the figures 7 and 8 show the distribution of the maximum forces on the collision devices.
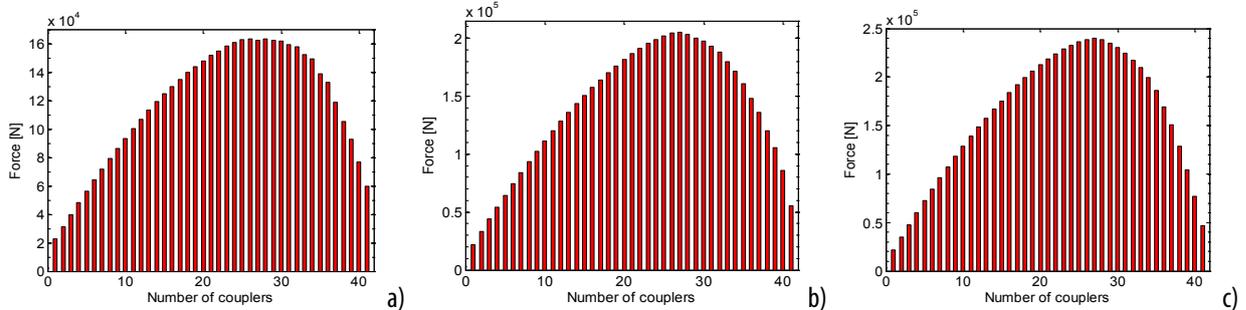

Figure 7. Maximum compression forces for the Lo-40W-Lo train.
a) the weight of a wagon is 50t, b) the weight of a wagon is 65 t; c) the weight of a wagon is 80t.
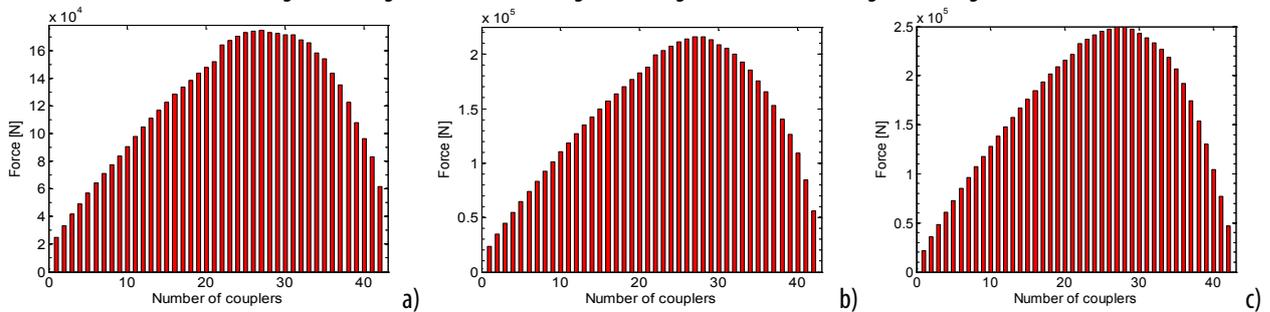

Figure 8. Maximum compression forces for the Lo-20W-Lo-20W-Lo train.
a) the weight of a wagon is 50t, b) the weight of a coach is 65 t; c) the weight of a wagon is 80t.
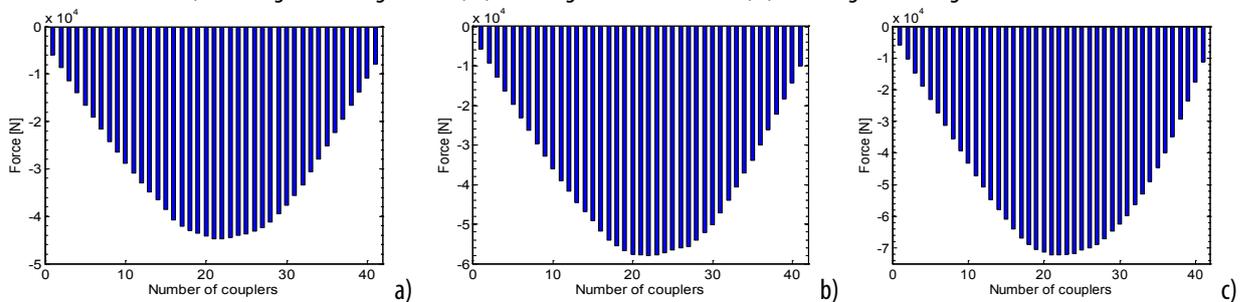

Figure 9. Maximum extension forces for the Lo-40V-Lo train.
a) the weight of a wagon is 50t, b) the weight of a wagon is 65 t; c) the weight of a wagon is 80t.
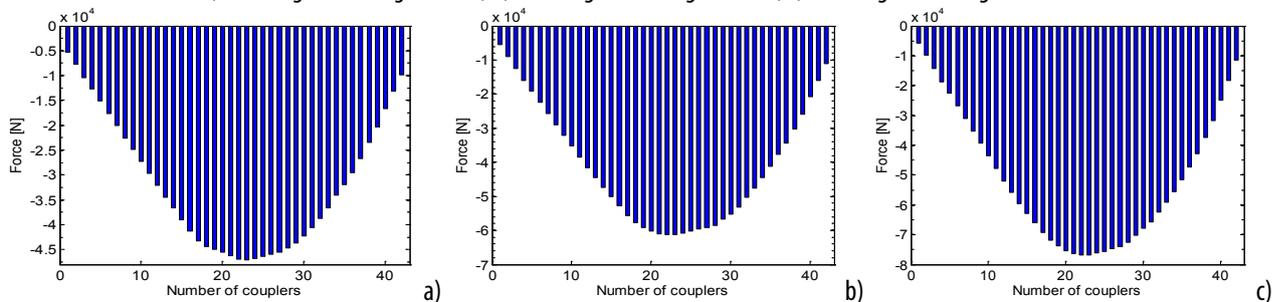

Figure 10. Maximum extension forces for the Lo-20V-Lo-20V-Lo train.
a) the weight of a wagon is 50t, b) the weight of a wagon is 65 t; c) the weight of a wagon is 80t.

Upon examining the compression forces derived from the simulations performed on the Lo-40W-Lo train, the conclusions are as such:
✓ The maximum extension forces are to be found in the second half of the train (the most stressed buffers are the ones between 24 and 32);

✓ The increase in the tonnage to be towed (by raising the weight of the wagons from 50 t to 65 t and to a final 80 t) will trigger the increment of the compression forces from 164 kN to 240 kN;

✓ For low tonnages (the present case of 50 –tone coaches) the compression force is noticed to increase on the last group of buffers (located between the last wagon and the push locomotives). The explanation is the very large weight introduced by the locomotives, compared to the wagon weight. When the wagon weight goes up (80 t per coach), the compression force on this collision device lowers by up to 25%.

The installation of the push locomotive in the middle of the train means a sudden increase in the compression forces, starting with the collision device number 22. This aspect is evident in fig 8a where, due to the low weight of the wagons, compared to the locomotive's, the force on this buffer increases by 5.5%, versus the case with no locomotive in that position.

Upon examining the results for the two types of trains (fig 7 and 8), the observation is that the installation of a locomotive in the middle of a freight train will lead to a higher maximum level reached by the compression forces with circa 10 kN.

The maximum extension forces that develop on the traction and coupling equipment show at the level of devices 21…24, reaching values between 44 kN and 72 kN (Figure 9 and 10). In terms of the distribution of the extension forces, there is an approximately symmetric distribution with maximum forces in the middle of the train, while the minimum ones show at its ends.

6. CONCLUSIONS

The use of the trains with multiple traction is a common practice among the freight trains operators. This paper examines the dynamic effects that an emergency braking can have within the body of the trains with multiple traction. Two train configurations are considered, with two and three locomotives, respectively (one is intermediary).

Following the numerical simulations, the below conclusions can be agreed on:

✓ the weight of the wagons in the train body has a major contribution upon the longitudinal dynamic forces developed in the traction, collision and coupling devices during braking;

✓ the increase in the tonnage to be towed (by changing the weight of the wagons from 50 t to 80 t) will lead to higher compression forces of up to 46% and extension forces of up to 60%;

✓ the installation of an locomotive at the end of the train will trigger an increase in the force on the last group of buffers. On the other hand, should the tonnage goes up by 60%, the force on this group of buffers lowers to up to 25%;

✓ the installation of a push locomotive in the middle of the train will result into a bounce of the compression forces on the buffers between this locomotive and the next wagon and the maximum values of the forces will increase by up to 4.2% compared to the case without locomotives within the train body.

The future research will have to consider a series of issues not dealt with in the paper herein, such as the influence of the block brake upon the longitudinal dynamic forces in the freight trains.

References

[1.] Duncan, I. B. and Webb, P. A., The Longitudinal Behaviour of Heavy Haul Trains Using Remote Locomotives, Fourth International Heavy Haul Conference, Brisbane, pp. 587 –590, 1989.

[2.] Jolly, B., J., Sismey, B., G., Doubling the Length of Coals Trains in the Hunter Valley, Fourth International Heavy Haul Conference, Brisbane, pp. 579 –583, 1989.

[3.] Nasr, A. & Mohammadi, S., The effects of train brake delay time on in-train forces, Proc. IMechE Vol. 224 Part F: J. Rail and Rapid Transit, pp. 523-534, 2010.

[4.] Cole, C., Longitudinal train dynamics, chapter 9 in Handbook of Railway Vehicle Dynamics, edited by Simon Iwnicki, Ed. Taylor & Francis Grup, pp. 239-277, 2006.

[5.] Fukazawa, K., Coupler forces of 1000t class two-axle freight trains. Q. Rep. RTRI, Vol. 33, pp.166–168, 1992.

[6.] Zobory, I. and Békefi, E., On real-time simulation of the longitudinal dynamics of trains on a specified railway line. Period. Polytech. Transport. Eng., Vol. 23, pp.3–18, 1995.

[7.] Ansari, M., Esmailzadeh, E., Xounesian, D., Longitudinal dynamics of freight trains, Internaţional Journal of Havy Vehicle Systems, ISSN 1744-232x, DOI 10.1504/IJHVS.2009.023857, Vol. 16, No. 1-2, pp. 102-131, 2009.

[8.] Pugi, L.; Fioravanti, D. & Rindi, L., Modelling the longitudinal dynamics of long freight trains during the braking phase, 12th IFToMM World Congress, Besançon (France), June18-21, 2007.

[9.] Stoica, M., Contribuţii la dinamica frânării trenurilor la tonaje şi viteze sporite, Teză de Doctorat, Bucureşti, 1998.

[10.] Sârb, M., Studiul dinamicii longitudinale la trenurile de marfã, Teză de Doctorat, Bucureşti, 2005.

[11.] Fiche U.I.C. Nr. 526-1: Wagons-Buffers with a stroke of 105 mm, 3rd edition, ISBN: 2- 7461-1463-1, July 2008

[12.] Craciun, C., Mazilu, T., Simulation of the longitudinal dynamic forces developed in the body of pasangers trains, Annals of Faculty Locomotiveering Hunedoara, International Journal of Locomotiveering, Tome XII, Fascicule 3, ISSN 1584-2673, pp. 19-26, 2014.

[13.] Cruceanu, C., Train Braking, book chapter in the book "Reliability and Safety in Railway" edited by Xavier Perpinya, InTech, 2012.

[14.] *** Instrucţiuni privind revizia tehnică şi întreţinerea vagoanelor în exploatare. Nr. 250, Ministerul Transporturilor Construcţiilor şi turismului, ISBN 973-86627-6-1, Ed. Feroviară, Bucureşti 2005.

[15.] Fiche Nr. 540: Freins à air comprimé pour trains de marchandises et trains de voyageurs, 3e édition 1982, U.I.C., Modificatif 1992.

[16.] Craciun, C., Contribution on the dynamic phenomena wich occur durimg train braking, doctorat thesis, Bucharest, 2014.